MOTOR WINDING PROBLEMS

Caused by Inverter Drives

An investigation intoSTATOR WINDING FAILURES caused by the VOLTAGE SURGE ENVIRONMENT.

By Mark Fenger, Steven R. Campbell, & Jan Pedersen

From IEEEIndustry Applications Magazin, July/August 2003, Pages (22–31)

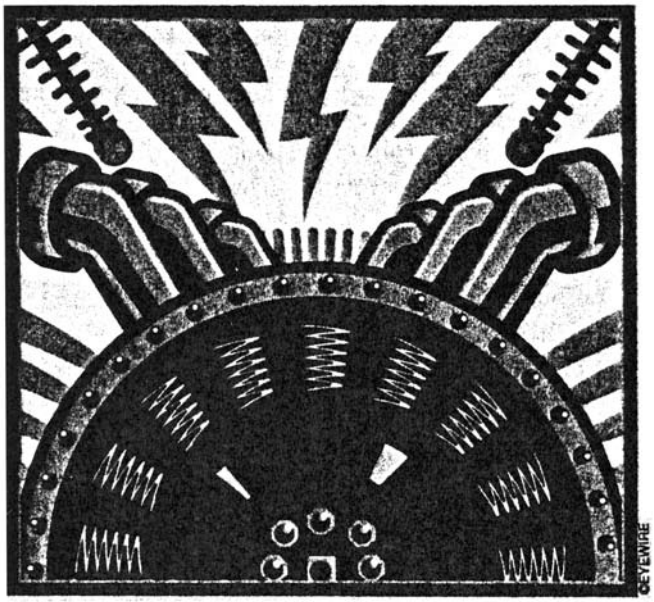

FOR OVER 70 YEARS, RESEARCHERS have understood that fast rise-time voltage surges surges from a circuit breaker closing can lead to an electrical breakdown of the turn insulation in motor srator windings [1]. If the turn insulation is of an insuffcient thickness or has aged in service, the insulation will puncture when a short rise-time voltage surge occurs. Punctured turn insulation allows for a very high circulating current to flow into the affected copper turn, rapidly melting the copper conductors, which, in turn, results in a consequent burning/melting of the slot liner insulation, thus leading to a stator winding ground fault [2], [3].

Rapid advances in power electronic components in the past decade have lead to a new source of voltage surges. Inverter-fed drivers (IFDs) of the pulse width modulated (PWM) type that use insulated-gate bipolar junction transistors (IGBTs) can create tens of thousands of fast rise-time voltage surges per second. Anecdotal evidence suggests that the large number of voltage surges from IFDs can lead to gradual deteriorations and eventual failure of the turn insulation—both in low voltage (less than 1,000V) and medium voltage (2.3 to 4.16kV) motors [4]–[6].

This article describes measurements of the surge voltage characteristics from a group of eight low-voltage motors driven by IFDs. As described here, two motors have repeatedly been subjected ro unexpected stator winding failures. Inspection of the windings after failure indicated that the main cause of the failures is the voltage surge environment applied to the stator winding.

The Impact of Voltage Surges on Low-Voltage Stator Winding Insulation

An investigation of the surges applied to random wound stator windings by IFDs show that these surges may have frequency components up to 5 MHz or so. At such frequencies, the stator windings appear as a complex ladder network with low-impedance capacitive shunts to ground. The capacitive shunrs cause most of the applied surge voltage to be dropped across the first few curns in a stator winding.

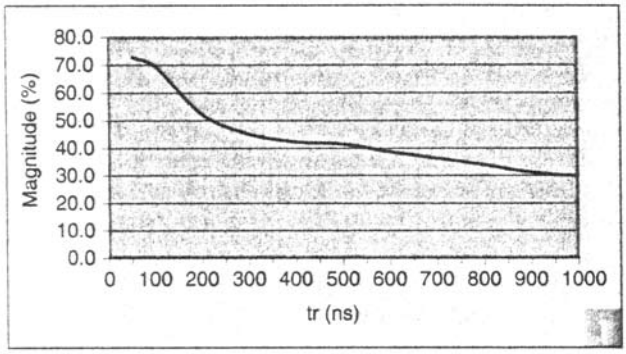

Voltage drop across first coil versus surge rise-time in a small random wound motor.

By injecting a 5-V pulse from a variable rise-time pulse generator (HP 8012) into a sraror winding and measuring the voltage across the first turnwith a differential very **low** capacitance probe, measurements were conducted co experimentally determine the amount of voltage chat appears across the first turn in a stator winding as a function of the voltage rise-time (Figure 1). As much as 75% of the surge voltage applied to the terminals can be distributed throughout the first coil.

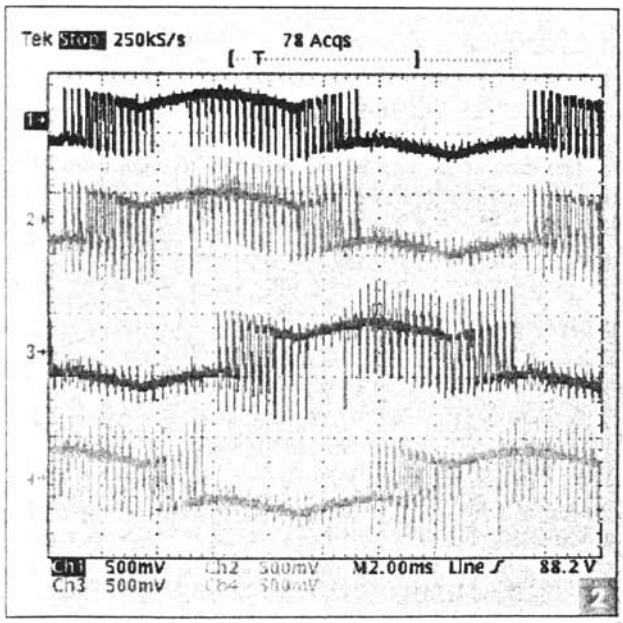

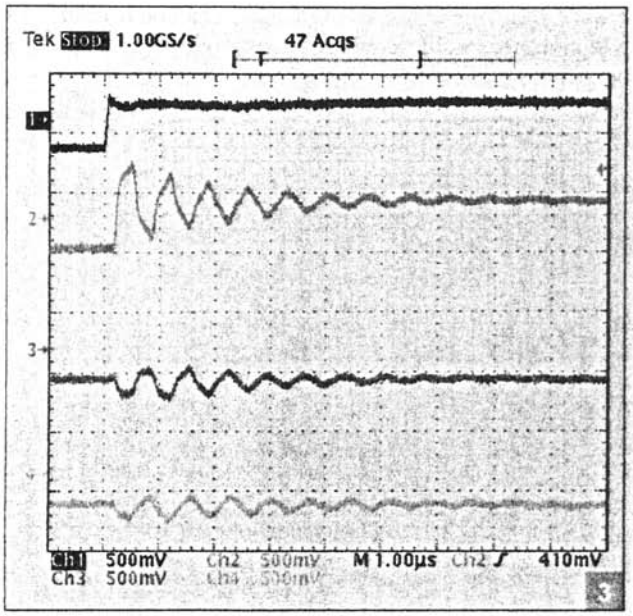

Furthermore, Figure 1 shows that the voltage distributed across the first coil, relative to the surge magnitude, is inverse proportionate to the rise-time. The higher the voltage across the first turn, the higher the risk of a partial discharge (PD). Consequently, fast rise-rime surges of higher magnitudes have a high risk of inducing PD in the random wound stator winding.

Figures 2 and 3 show the surge waveform measured at the terminals of a 10-hp, 440-V squirrel cage induction motor fed by a 600-V PWM-cype of drive that uses IGBTs. The waveforms were measured via an oscilloscope using low inductive resistive voltage dividers attached at the motor drive and the motor terminals. There is about 30m of shielded triplexed power cable between the drive and the mocor. This drive created 10,000 surges per second. The recorded waveforms had riserimes as short as 80 ns. The highest magnitude recorded was about 1,200 V, or about 3.3 per unit, with 1 per unit corresponding to the raced peak line-to-ground voltage of the motor. In Figures 2 and 3, the top trace is the A-phase signal at the drive. The other three traces are at the motor. The scope was in peak hold mode.

Figure 2, which shows a: full ac cycle of applied voltage, shows char there is much more ring overshoot at the motor terminals, resulting in bipolar surges of varying magnitudes. Thus, in order to characterize the surge environment, surge measurement must be carried out at the motor terminals and not at the drive;
Furthermore, Figure 3 shows that one surge from the drive can create several surges at the motor terminals of different rise-times and magnitudes. Hence, the stator windings are subjected to a *distribution* of surges.

Thus, Figure 1 shows the shorter the rise-time, the greater the voltage across the first rum and the more dangerous the surge becomes ro the motor. Therefore, by fully characterizing the surge environment applied to a random wound Stator winding, one can assess the risk of stator failure due to electrical degradation.

Finally, as outlined in [121, the measured surge environment may be assessed quantitatively by performing PD inception voltage (DIV) measurements as a function of rise-time for the srators examined. By superimposing the DIV curve on the measured surge plot, the surge plot is essentially calibrated with reference to which surges may give rise to PDs.

Surge Measurement System

As described earlier, IFDs create tens of thousands of voltage surges per second, with varying magnitudes and rise times as fast as 50 ns. The voltage surges from an IFD pulse applied at the sraror terminals may be measured by conventional means via a simple resistive voltage divider and a digital oscilloscope. This system allows for the measurement of the waveform of a given surge.

However, as discussed in [II], digital oscilloscopes exhibit an inherent limitation when used for recording surges: A vase majority of surges are ignored since a digital oscilloscope can only be triggered from 1-10 times per second, while 20,000 surges may occur in the same interval Hence, only one in about 1,000 surges can be recorded. In addition, the oscilloscope can normally only be triggered on the largest magnitude surges. As moderate magnitude surges with very fast rise-times may be more damaging to the scator insulation than high magnitude/slow rise-time surges, it is likely that the oscilloscope may not trigger on the surges which, in time, are most likely to cause insulation failure.

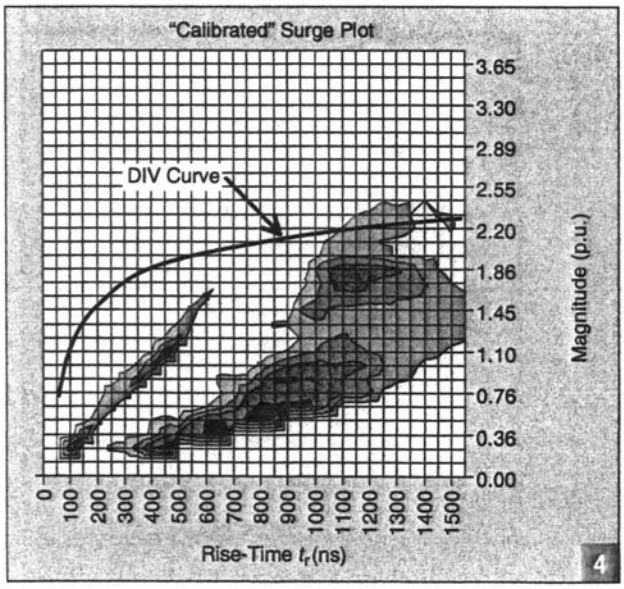

Example of a calibrated surge plot [12].

In order to assess the severity of the electrical surge environment in which a motor operates, a reliable measurement of the distribution of electrical surges must be performed. The distribution of surges is defined by the magnitude, rise-time, and repetition rare of each surge applied to the stator. When the exact surge environment is known, the surge distribution is said to be characterized. Thus, the surge environment cannot be characterized via conventional means.

To overcome the limitations outlined below, a special electronic instrument was developed. This device, SurgAlert, measures the magnitude and rise-time of every surge that occurs within a given time interval. It also determines the total number of surges that a motor is subjected to during the measurement interval (Figure 4). However, this instrument cannot record the entire waveform of each surge. The monitor has the following specifications:

- wideband (50 Hz to 10 MHz) resistive or capacitive voltage dividers, capable of operating on motors rated up to 13.8 kV (For motors rated 600 V or less, a resistive voltage divider is used. The dividers must be installed at the motor terminals.)
- a portable electronic instrument, which is temporarily placed near the motor for the duration of the measurement, that digitally records the rise-time and magnitude of each surge and stores this information in memory
- a laptop computer that downloads a summary of the measured surges recorded in the measurement interval, for display or printout.

The data acquired may be exported to a computer file that is readable by Microsoft Excel. Thus, it is possible to perform further processing of the data acquired. Further details of the surge monitoring system are given in [7].

TABLE 1. OVERVIEW OF TESTED MOTORS.

Motor	Application	Power Rating [kW]	Rated Voltage [V]	Drive Model	Cable Type	Cable Length [m]
1	Main cooling pump	850	690	SVTL 1K2	XLPE	131
2	Condensation pump	680	690	SVTL 840	XLPE	114
3	Drain pump	130	690	SVTL 210	XLPE	75
4	Small pump	500	690	SVTL 600	XLPE	15
5	Main condensation pump	485	690	SVTL 600	XLPE	45
6	Main condensation pump	485	690	SVTL 600	XLPE	53
7	Big pump	1890	690	SVTL 2K4	XLPE	33

TABLE 2. FAILURE TIMES FOR MOTORS 1 AND 3.

Motor	Application	Power Rating [kW]	Date of fault	Total operating hours	Number of starts
1	Main cooling pump	850	10-06-1998	2,140	4
			10-02-2000	13,044	119
			14-09-2000	13,177	152
2	Condensation pump	680	13-10-2000	9,440	753

In-Service Failures Due to IFDs

The following data was obtained from motors located in a combined power and district heating plant. The net electrical output is 390 MW. The plane was put into operation in July 1997. A large number of variable-speed drives have been installed for operation of pumps co reduce the unit's house load. Motors raced 90 kW (120 hp) and below are mainly supplied from the 400-V busbar, whereas motors rated above 90 kW (120 hp) are supplied from the 690-V bus bars. A roral of nine motors, of which seven participated in this survey, are supplied from the 690-V bus bars. The size of these motors vary from 130 kW (175 hp) up to 1,890 kW (2,520 hp). All seven motors and their inverters are from the same

Picture of Motor 1 after failure.

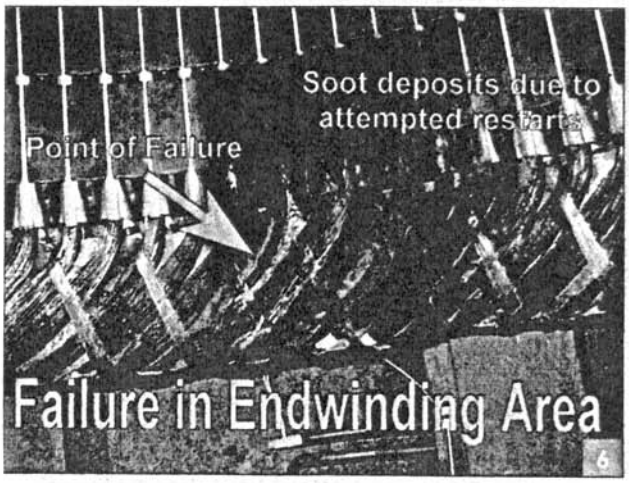

Close up of Motor 1 failure.

supplier. The basic data for the motors participating in this survey is given in Table 1.

Since the commisioning, two of the seven motors have been subjected to stator winding failures. One motor (850W) failed three times within the first 36 months of service, and another motor (680 kW) failed once after 36 months. On the motor that failed three times, the third failure occured after less than six days of service. Operating hours and the number of starts for the two motors that failed are given in Table 2.

After the first failure on Motor 1 (Figures 5-7), the motor manufacturer was confronted with the sugges tion that fast rise-time voltage surges originating from the IGBT inverter may have lead to the premature winding failure. This theory was rejected by the manufacturer who came to the conclusion that the failure was accidental and that a similar failure would quite unlikely occur again.

Following the second failure on the same motor, the theory of fast rise-time voltage surges being the cause of failure was brought up again. Once more, this theory was rejected by the manufacturer. As before, the conclusion was that the failure was accidental. However, the manufacturer agreed to perform on-site voltage measurements at the motor terminals in order to assure the customer that the failure was accidental and not caused by voltage surges. These measurements were performed only two days before the third failure on the same motor occurred.

One month later, a second motor failed. This failure lead to the decision to perform an independent measurement of the electrical surge environment on all 690-V motors using the surge monitor.

Although both motors that failed were still covered by the manufacturer guarantee, the unforeseen failures have lead to considerable expense co the power station

Motor/IFD Configuration

The basic data for the motors participating in this survey is given in Table 1. The following information on the specific winding design is given by the motor manufacror:

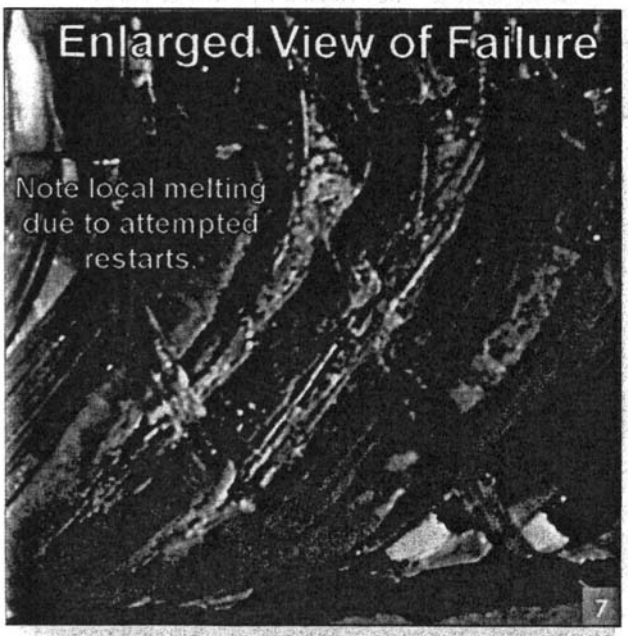

Enhanced close up of Motor 1 failure. Local melting of the stator winding is clearly visible.

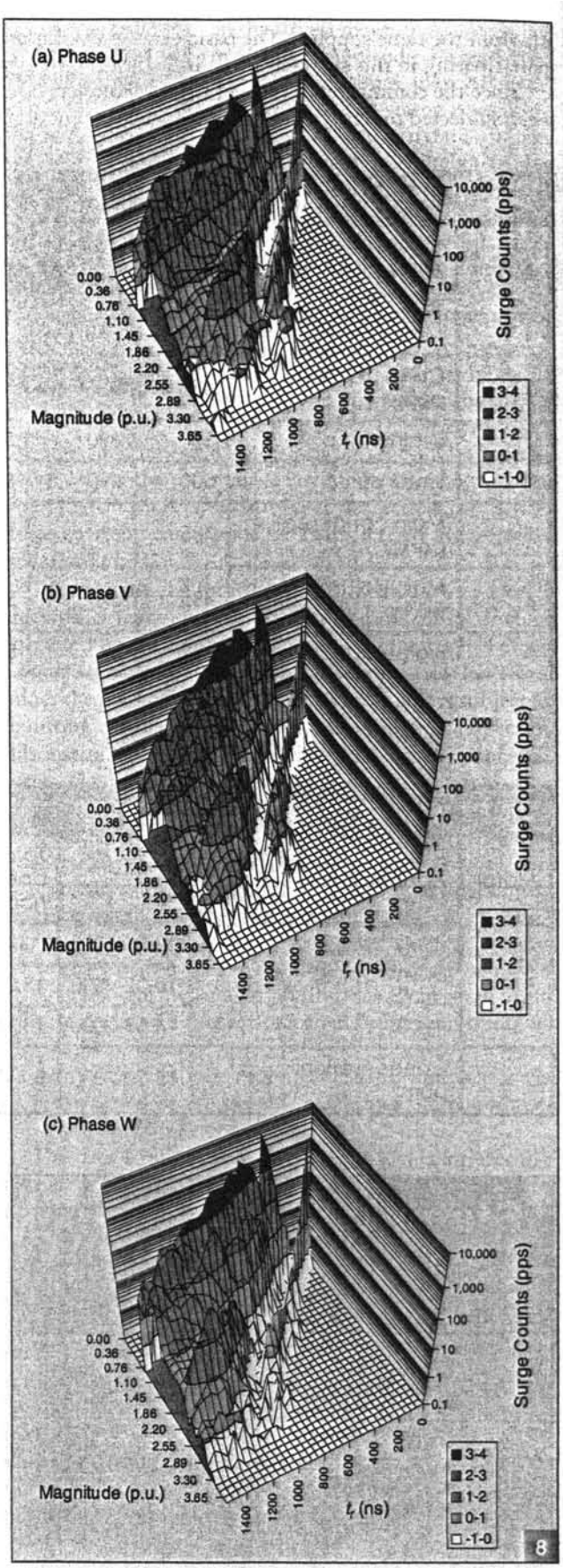

Surge Environment for Motor 1. (a) Phase U. (b) Phase V. (c) Phase W.

• the round wire is insulated with a quadruple build, Class-H enamel
• the coils of different phases are completely separated with mica paper on the overhangs
• all the coils are separated with mica paper on the nose area

• in the slots, the coils are insulated to ground and between each other with layers of NOMEX

• the winding is vacuum-pressure impregnated (VPI) in a special blend of Class-H, flexible, and thixotropic resin.

The resin was oven cured and the stator turned while in the oven. Such a process gives an even coverage on the over-hangs.

The motor manufacturer insists that random wound mocors with the above described specific design can be used for this type of application. Nevertheless, motors supplied for similar applications at another power station of the same utility in 1999 were delivered with form-wound winding construction.

Measurement Procedure

By attaching a very low inductance resistive voltage divider to the motor terminal of a given phase, a measurement of the surge environment of each phase could be performed. A three-dimensional (3-D) surge plot characterizing the surge environment applied to that phase could thus be created.

Using alligator clips to connect to the motor terminals provides an easy and quick way to perform a measurement. The alternative is to temporally install low-inductive voltage dividers prior to performing the measurements. This ensures chat the protection equipment will not trip the motor due to slight voltage imbalances between phases due to the increased load (from the instrument) on one phase. This option is more time consuming, as it requires down time to install each voltage divider and, in most cases, is not technically necessary. However, local plant regulations may or may not allow for connecting a probe during normal online operation.

First, two measurements were performed on the same phase of a motor: a 5-s measurement and a 10-s measurement. By normalizing the surge counts for each measurement into surge counts per second, a direct comparison between the two tests can be made.

This procedure allows for investigation of the consistency of the surge environment applied to the stator winding. If the surge environment is consistent, only one test is needed per phase to fully characterize the surges applied to the staror winding. This issue is discussed later in this article.

The output is plotted as a 3-D curve (Figure 8), with the left scale being the magnitude of the voltage per unit (1 p.u. is the peak line-ground rated voltage), the bottom scale is the rise-time of the surge in nanoseconds, and the vertical scale indicating the number of surges per second for each combination of surge magnitude and rise-time. Note that this is a log scale.

Often, a two-dimensional (2-D) representation of the 3-D plot is used (Figure 9). A color scheme thus provides information on the surge count rate. As described earlier, the surges most likely to cause winding failure will have a short rise-time and high magnitude, that is, they will appear in the lower right part of the

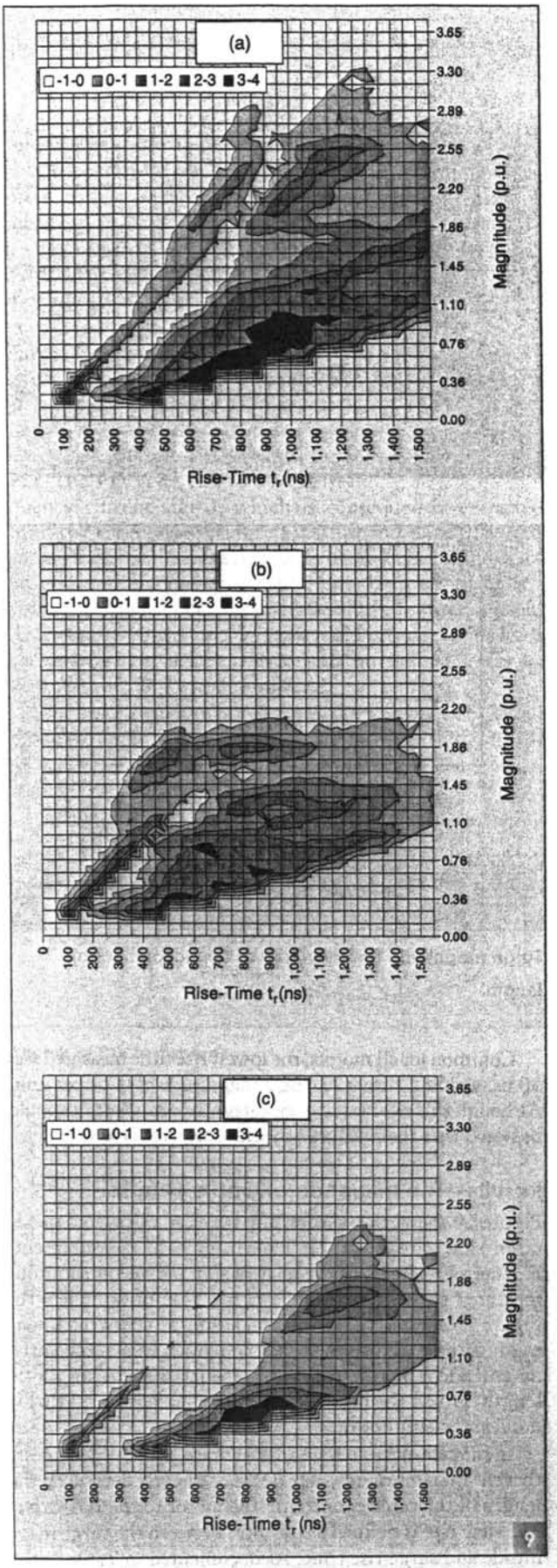

2-D surge motor plots for motors (a) 1, (b) 2, and (c) 5.

3-D plot. A 2-D representation allows for quick identification of these.

Results—The Difference Between Phases

All phases were tested for all motors. The measurements showed that the surge environment measured on one phase was very similar to that measured on the remaining two phases. Figure 8 shows the surge plots for phases U, V, and W of Motor 1.

As can readily be seen, there is no significant difference in the surge environment applied to each phase of the stator winding. This is hardly surprising as, from a theoretical point of view, the surge environment is defined by the output of the IFD drive.

The plots of Figure 8 are typical of chose obtained on alt eight motors tested, i.e., no significant differences in the surge environment could be detected between phases of a machine.

Furthermore, both 5- and 10-s rests were performed. Both tests were normalized ro a 1-s rest. A comparison between these tests showed similar surge distributions for the 5- and 10-s test, which is indicative ot consistent surge environment.

Hence, for interpretational purposes, only one measurement per phase is needed to address the severity of the surge environment applied to a given sraror winding.

TABLE 3. RESULT SUMMARY OF TESTS.

Motor	Maximum Magnitude [p.u., ns]	Fastest Risetime [p.u., ns]	Max Slew Rate [p.u./ns]
1	3.51, 1,500	0.24, 50	5.1
2	2.34, 900	0.24, 50	6.0
3	3.09, 1,400	0.24, 50	5.3
4	2.20, 900	0.24, 50	5.3
5	2.41, 1,100	0.24, 50	3.8
6	2.41, 1,100	0.24, 50	4.0
7	1.44, 950	0.24, 50	3.7
8	2.41, 700	0.24, 50	5.8

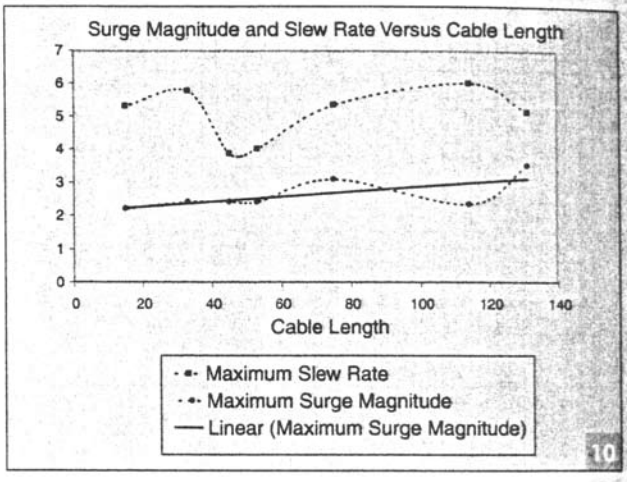

Surge magnitude and slew rate as a function of cable length.

Results—Comparative Analysis

An initial inspection of Table 3 clearly shows Motors 1 and 2 to be subjected to the highest surge environment in terms of pulse count rates and pulse magnitudes. The highest surge magnitude measured on Motor 1 was 3.5 per unit at a rise time of 1,500 ns, whereas the highest surge magnitude measured on Motor 2 was 3.1 per unit at a rise time of 1,400 ns. Fortunately, these high surge magnitudes are measured at relatively high rise-times. Such high magnitude surges should not be too damaging co the insulation. However, an investigation of the 2-D plot for Motor 1 reveals the presence of a series of surges having rise-times of 100-650 ns, with magnitudes ranging from 0.25 to 2.2 per unit and repetition rates of 1-10 and 10-100 pulses per second (Figure 9). The presence of these pulses is more of a concern than the presence of the maximum magnitude pulses of 3.5 per unit at a rise time of 1,200 ns, having a repetition rare of 1 per second. As mentioned earlier, the faster the rise time, the higher the electrical stress between turns or phases. Hence, although not being of alarmingly high magnitudes, the faster rise time pulses measured on Motor 1 may be of a concern with respect to aging of the Stator insulation.

Furthermore, the 2-D plot indicates two types of surges: initial surges created by the IFD and secondary surges possibly created by resonance phenomena. This is indicated by the general separation of surges into two “islands” in the plot (Figure 9). The surge environment measured on Motor 1 constitutes the most significant surge environment measured so far using the SurgAlert technology. The data showed that similar observations can be made for Motor 3.

Table 3 shows that the highest slew rate measured for Motor 1 is 5.1 and 5.3 for Motor 2. These slew rates can be classified as being moderately high compared to the highest slew rate of 8.1 per unit measured so far on other machines elsewhere.

The surge environment for Motor 2 is also given in Figure 9 and can be characterized by a maximum pulse magnitude of 2.34 per unit at a rise time of 900 ns. The measured slew rate is six and constitutes the highest slew rate measured on these motors. As such, it can be argued, from a general point of view, that this motor is subjected to the “worst” surge environment of all the motors measured in this rest. An investigation of the surge plot shows the initial surges for Motor 2 to have noticeably higher repetition rates than those measured for Motors 1 and 3.

The surge environments measured for the remaining five motors are, without doubt, of less concern. As can be seen from Table 3, the maximum surge magnitudes measured are noticeably lower than those measured on Motors 1, 2, and 3. This is consequently expressed in the 2-D surge plots—an example from Motor 5 is given in Figure 9. The slew rates, however, appear ro be moderately high for the remaining five motors, with Motor 6 yielding a slew rate of four. This is the lowest slew rate detected for the eight motors measured in this test.

Common for all motors, the lowest rise time measured was 50 ns, yielding surges having a magnitude of 0.24 per unit. Although this rise time can be categorized as short, it should be noted that the measured magnitude is relatively low.

Results—The Influence of Cable Length

Figure 10 shows the relationship between calculated maximum slew rare and cable length for each measurement. Furthermore, it shows the relationship between maximum measured surge magnitude as a function of cable length. Figure 10 suggests that

a clear relationship between maximum surge magnitude and cable length exists: the surge magnitude appears to increase with increasing cable length. Given the nature of traveling-wave theory, this is not a surprising result.

In the case of the maximum slew-rate. Figure 10 suggests that the maximum slew-race does not directly depend on the length of the cable connecting the motor to the IDF drive. The slew rate is defined as the ratio between che surge magnitude and surge rise time. As documented in Table 3, the rise-times measured for the maximum surge magnitudes range from 700-1,500 ns, thus giving rise to an erratic distribution of slew-rates for increasing surge magnitudes. Thus, Figure 10 suggests cha the slew-rare is a secondary effect of the cable length; it cannot be concluded that the longer the cable length, the more damaging the surge environment is.

PD Inception Voltage

The basic principle of the test setup is sketched in Figure 11. Via a Baker Surge Tester, Model D12000, a 50-ns rise-time surge voltage is applied to an insulation sample or a staror winding. If it is of sufficient magnitude, the surge voltage will give rise to a PD. The PD gives rise co a high-frequency current signal, which is consequently extracted from the surge via specialized instrumentation, PDAlerr, connected in series between the surge source and the insulation sample. The net output from the instrument is a voltage signal originating from the PD current pulse itself. An example from Motor 1 is given in Figure 12. The leads connecting the various components of the rest secup are kept as short as possible.

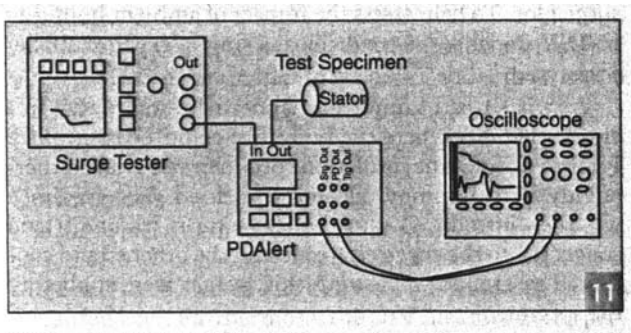

Sketch of DIV test setup.

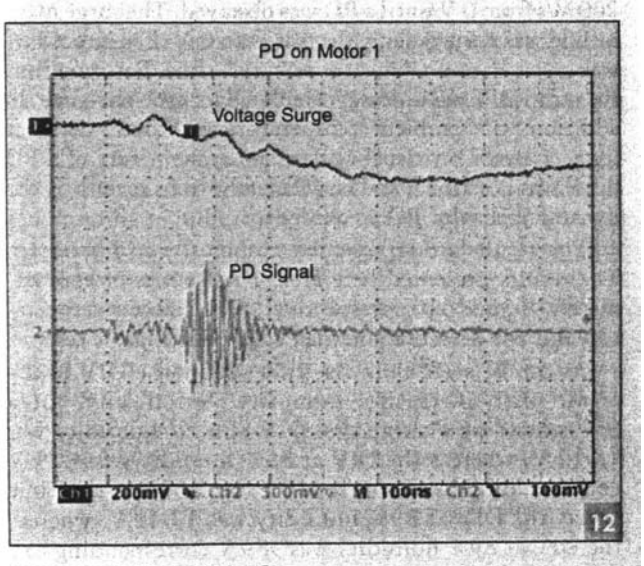

Example of PD on Motor 1.

The test procedure is described thoroughly in [12] but repeated in short here: Having connected a scaror to the surge source, the surge magnitude was increased with approximately 200 V/'s from 0 V until a PD was observed. The surge magnitude was then quickly decreased co 0 V. The procedure was repeated seven times for each rise-rime. Based on this, the mean (average) DIV was calculated for each rise-time. In addition, the Jmbient temperature and humidity, was logged.

Results—PD

The average discharge inception voltage was 1.73 per unit for Motor 3. For Motor 1, the average DIV was 2.38 per unit. Table 3 shows that the maximum magnitudes—of surges having rise times up to 1,550 ns—is below the DIV for these motors. This strongly indicates that these motors are subjected to PDs, during normal operating conditions, due to the surge environment applied to the staror windings from the IFD and the connection cables.

A curve of the DIV versus rise-time for Motor 1 is given in Figure 13. The curve shows the DIV ro decrease with decreasing rise-time. This is surprising, as other curves obtained on new scacors prior to being put into service shows the opposite relationship, namely an increase in DIV with increasing rise-time as explained by the distribution of voltage across the first turn as a function of surge rise time.

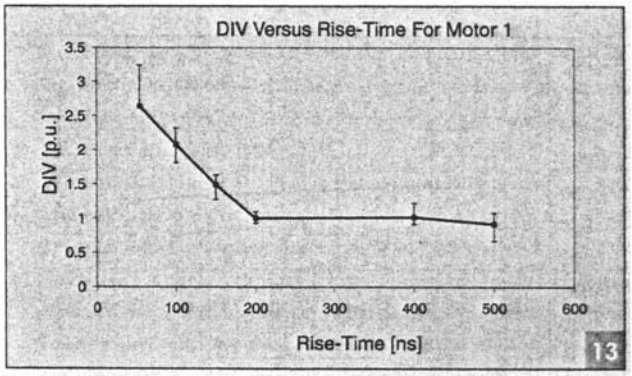

Discharge inception voltage versus rise-time for motor 1.

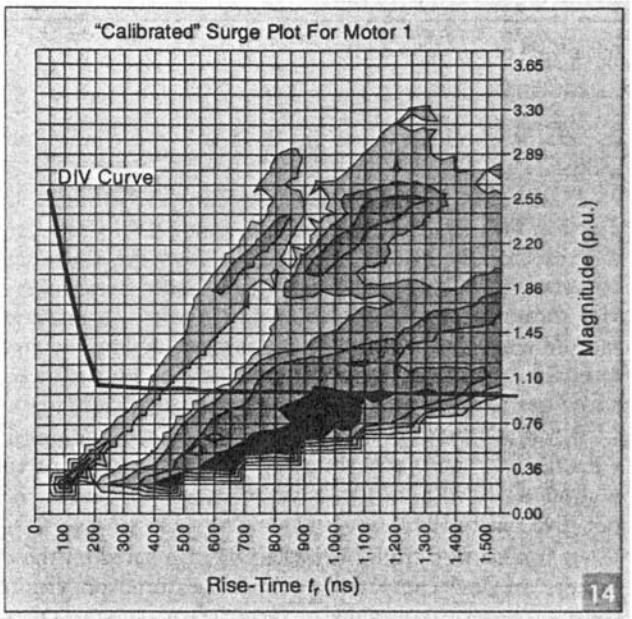

Calibrated surge plot for Motor 1.

Figure 14 shows the measured surge plot for Motor 1 with the DIV curve superimposed. Surges above the curve may give rise to PD.whereas surges below the curve will not give rise to PD.

As can be seen from [12], the DIV measured on these motors are low compared to those measured on virgin stators. The results

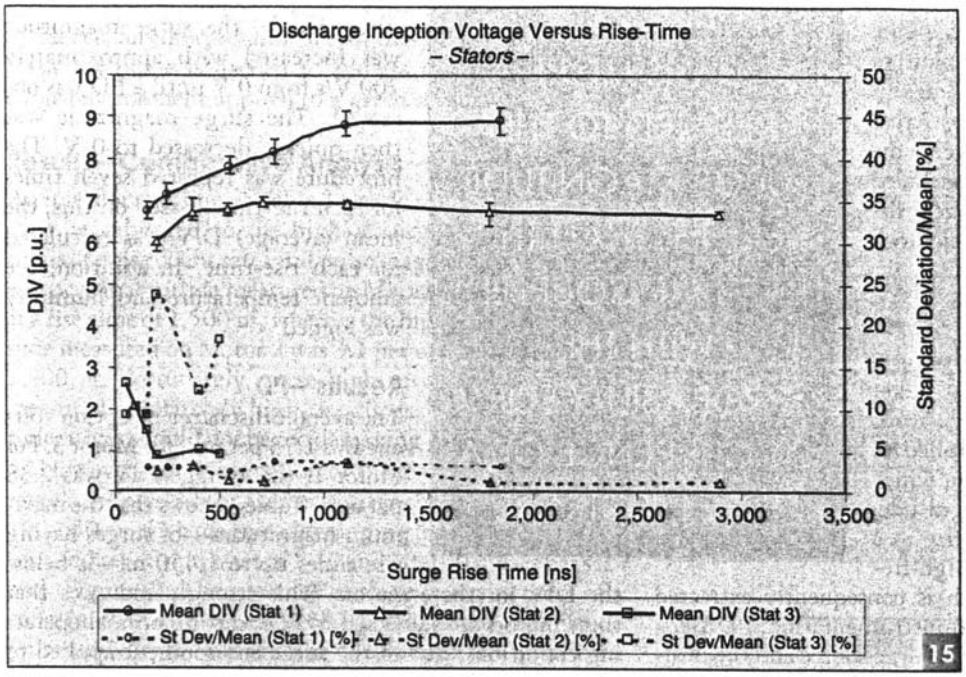

DIVs for motors of different design and size [12].

obtained on virgin srators showed DIVs of between 6 to 9.5 per unit—as seen from Figure 15, where Srators 1 and 2 are virgin stacors, and Staror 3 constitutes the DIV for Mocor 1 [12].

Compared to the results obtained on virgin windings and presented in [12] these results indicate that for aged windings (i.e.,windings subjected to real operating conditions), DIV is more related to the surge magnitude rather than the rise-time coupled with the probability for occurrence of a free electron, which increases with increasing (slowing) rise-time.

The Impact of Humidity on the Measured DIV

As mentioned earlier, the surge environment is characterized during normal operating conditions, i.e., at a given stator winding temperature and ambient humidity. However, ambient humidity may have an impact on the measured DIV and, thus, an impact on the interpretation of the calibrated surge plot. To help assess the impact of ambient humidity on DIV under surge conditions, a simple experiment was performed.

A twisted-pair sample of magnet wire was placed in a closed chamber where the humidity could be controlled. Prior to testing, the insulation specimen was cleaned thoroughly with isopropyi alcohol and dried. The specimen was then introduced into the test setup with one strand connected to the surge electrode and the other strand connected to ground. Following this, surges were applied to the specimen.

The surge magnirude was increased at approximately 200 V/s from 0 V until a PD was observed. The surge magnitude was then quickly decreased to 0 V. The procedure was repeated seven times for each rise-time. Based on this, the mean DIV per unit was calculated for each rise-time. In addition, the ambient temperature lind humidity was logged. Based on visual observations, the nature of a PD pulse was described, and visual observations regarding the dynamic behavior PD were logged.

The results are represented graphically in Figure 16. The results presented here are for rise times of approximately 960 and 510 ns respectively. The ambient temperature did not deviate more than 0.3 °C during the tests.

As can be seen, both rise times show the DIV to decrease with increasing humidity. Specifically, for a 967-ns rise-time surge, the DIV at 59% humidity was 1,012 V, whereas the DIV at 86% humidity was 929 V corresponding to a decrease of 8%. For a 5 l4-ns rise-time surge, the DIV at 39% humidity was 1,041 V, whereas the DIV at 89% humidity was 989 V corresponding to a decrease of 5%.

A theoretical discussion on the humidity results is given in [151 but will nor be repeated here. However, from a engineering point of view, based on these results, it can be stated that, although ambient humidity does have an impact on the measured DIV, the impact is not significant. Thus, the calibrated surge-plot obtained on-site using the measurement method presented here is valid and does help provide an assessment of the impact of the applied voltage surge environment co the random wound stator winding with respect to the occurrence of PDs.

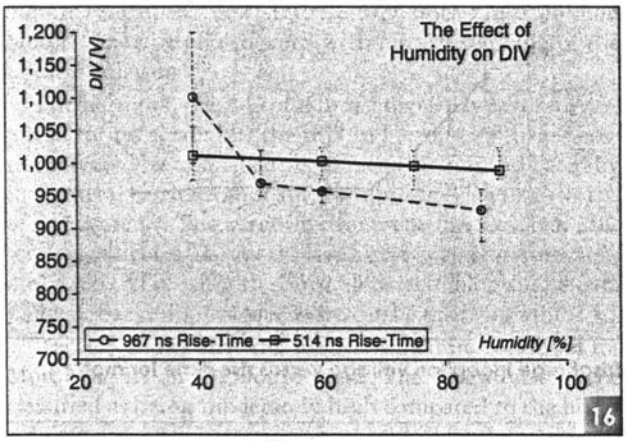

The effect of humidity on DIV.

Discussion

The measurements clearly showed Motors 1 and 2 to be subjected to a surge environment, which must be perceived as having a negative impact on the **stator** winding insulation and its estimated life time.

Confronted with the measurements performed using the SurgAlerr instrument, the motor manufacturers have accepted to supply and install filters on five of the nine motors. Filters have already been installed on the 850-kW motor that failed three times and will be installed on the remaining four motors as soon as possible.

Filters are simple 20-p.H reactors connected in series with the motor at the cable outlet from the inverter. The impact of these reactors is noc known at present. Preventive filters have been installed on Motors 1 and 3. Additional surge measurements are to be be performed once installed. Thus the measurements will clearly document the effect of the filters.

The DIV measurements strongly indicated that the surge environment applied to Motors 1 and 3 gave rise to PD activity.

Conclusions

The surge measurements clearly showed that the two motors that had previously experienced failures had been subjected to the worst surge environments of the motors measured here. Furthermore, the DIV measurements performed on Motors 1 and 2 clearly documented that the DIV, under surge conditions, were lower than the maximum surge magnitudes measured online during normal online operations. This Strongly indicates that the root cause of the failures experienced was indeed the presence of PDs.

Also, the measurements showed little difference in the applied surge environment between phases on the individual machines, indicating that, when performing these types of measurements, measuring one phase per motor should be sufficient.

Furthermore, when purchasing inverter drives intended fora690-V supply, the manufacturer should be asked to indicate acceptable surge levels at the motor terminals and required to perform measurements of the actual surge environment when the motors are being commissioned.

References

[1] E.W. Boehne, "Voltage oscillations in armature windings under lightning impulses," *TramAIE*E, p. 1587,1930.

[2] M.T. Wright, S.J. Yang, and K. McCleay, "General theory of fast-fronted inn;riurn voltage distribution in electrical machine windings, Pne. lust. Ehttr, Bug., Part B, p. 245, July 1983.

[3] B.K. Gupta, B.A. Lloyd, G.C. Stone, S.R. Campbell, D.K. Sharma, and N.E. Nilsson, "Turn insulation capability of large ac motors, parts 1, 2, and 3," IEEE Train, Energy Conversion, vol. 2, p. 658., Dec.1987.

[4] A.L. Lynn, W.A. Gottung, and D.R. Johnston, "Corona resistant turn insulation in ac rotating machines," in *Proc. IEEE Electrical Insulation Conf.,* Chicago, IL, 1985, p. *WS.*

[5] W. Yin, K. Bultemeier, D. Barta, and D. Floryan, "Improved magnet wire for inverter-fed motors," in Prat. IEEE Electrical Insulation Conf., Chicago, IL, 1997, p. 379.

[6] E. Persson, "Transient effects in applications ofPWM inverters to induction motors," *IEEE Trans. Ind. Applicat;* vol. 28, pp. 1095-1101, Sept./Oci. 1992.

[7] G.C. Stone, S.R. Campbell, and M. Susnik, "New tools to determine the vulnerability of stator windings to voltage surges form IFDs," in Proc. IEEE Electrical Insulation Couf., Cincinnati, OH, 1999, pp. 149-153.

[8] L.A. Saunders, G.L. Skibinslu, S.T. Evon, and K..L. Kempkes, "Riding the reflected wave—IGBT technology demands new motor and cable considerations," in IEEE Petroleum ana Chemical Industry Coaf. Rec., pp. 75-84, 1996.

[9] E.P. Dick, B.K. Gupta, P. Pillai, A. Barang, and D.K. Sharma, "Practical calculation of switching surges at moror terminals," *IEEE Trails. Energy Conversion,* vol. 3, pp. 864-872, Dec. 1988.

[10] C. Lanier, "A novel technique for the determination of relative corona activity within inverter-duty motor insulation systems using steep-fronted voltage pulses," in IEEE Int. Symp. on Electrical Insulation Conf. Rec., Arlington, VA, 1998, p. 229.

[11] G.C. Stone, S.R. Campbell, and S. Tetreault, "Inverter fed drives: Which motor stators are at risk?," IEEE Ind. Appl. .Mag., vol. 6, pp. 17-22,Sept. 2000.

[12] M. Fenger, S. R. Campbell, and G. Gao, "The impact of surge voltage rise time on PD inception voltage in random wound motors of different designs," in 2002 Annu. Report—Conf. en Electrical Insulation and Dielectrici Phenomena, p. 352.

[13] M. Fenger, G.C. Stone, and B.A. Lloyd, "The impact of humidity and surface pollution on PD inception voltage as a function of rise time in random wound motors of different designs," in *2002 Anna, Report—Conf. on Electrii:ai Insulation andDielectrics Phenomena,* p.501.

Mark Fenger (mfengtr@irispower.com) and Steven R. Campbell are with Iris Power Engineering Inc. in Toronto, Ontario. Canada. Jan Pedersen is with Techwise A/S in Fredericia, Denmark. Fenger and Campbell are Members of the IEEE. This article first appeared in its original form at the 2002 IEEE/IAS Cement Industry Technical Conference.